Molecular Biology of the Cell
Vol. 21, 2821–2831, August 15, 2010

Regulation of Exocytosis and Fusion Pores by Synaptotagmin-Effector Interactions

Zhen Zhang,* Enfu Hui,† Edwin R. Chapman,‡§ and Meyer B. Jackson§

*National Institute of Neurological Disorders and Stroke, Bethesda, MD 20892; †Department of Cellular and Molecular Pharmacology, University of California, San Francisco, CA 94158-2157; ‡Howard Hughes Medical Institute and §Department of Physiology, University of Wisconsin School of Medicine and Public Health, Madison, WI 53706

Submitted April 7, 2010; Revised June 2, 2010; Accepted June 15, 2010
Monitoring Editor: Patrick J. Brennwald

Synaptotagmin (syt) serves as a Ca^{2+} sensor in the release of neurotransmitters and hormones. This function depends on the ability of syt to interact with other molecules. Syt binds to phosphatidylserine (PS)-containing lipid bilayers as well as to soluble N-ethylmaleimide sensitive factor receptors (SNAREs) and promotes SNARE assembly. All these interactions are regulated by Ca^{2+}, but their specific roles in distinct kinetic steps of exocytosis are not well understood. To explore these questions we used amperometry recording from PC12 cells to investigate the kinetics of exocytosis. Syt isoforms and syt I mutants were overexpressed to perturb syt-PS and syt-SNARE interactions to varying degrees and evaluate the effects on fusion event frequency and the rates of fusion pore transitions. Syt I produced more rapid dilation of fusion pores than syt VII or syt IX, consistent with its role in synchronous synaptic release. Stronger syt-PS interactions were accompanied by a higher frequency of fusion events and more stable fusion pores. By contrast, syt-SNARE interactions and syt-induced SNARE assembly were uncorrelated with rates of exocytosis. This associates the syt-PS interaction with two distinct kinetic steps in Ca^{2+} triggered exocytosis and supports a role for the syt-PS interaction in stabilizing open fusion pores.

INTRODUCTION

With the increasing acceptance of synaptotagmin (syt) I and some of its isoforms as Ca^{2+} sensors for neurotransmitter release (Augustine, 2001; Koh and Bellen, 2003; Chapman, 2008), research on neurosecretion has turned to elucidating the mechanism by which Ca^{2+} binding to syt triggers membrane fusion. Syts have a large cytoplasmic domain containing two Ca^{2+}-binding modules, the C2A and C2B domains, each containing several acidic aspartate residues that coordinate the binding of Ca^{2+} (Shao *et al*., 1996). Early work on syt I showed that it binds to phosphatidylserine (PS)-containing liposomes in a Ca^{2+}-dependent manner (Brose *et al*., 1992; Davletov and Sudhof, 1993; Chapman and Jahn, 1994). However, Ca^{2+} binding to Syt I also promotes binding to soluble N-ethylmaleimide sensitive factor receptor (SNARE) proteins and complexes of SNARE proteins (Brunger, 2005; Chapman, 2008). Both of these interactions are essential for Ca^{2+}-dependent triggering of liposome fusion by syt I. Omitting PS from liposomes (Bhalla *et al*., 2005) and replacing synaptic SNARE proteins with yeast SNARE proteins prevented Ca^{2+}-syt I from accelerating liposome fusion (Bhalla *et al*., 2006). Increasing the PS content of PC12 cells increased the frequency of fusion events and stabilized fusion pores (Zhang *et al*., 2009). Thus, although both of these Ca^{2+}-triggered interactions play some role in neurotransmitter release, their precise functions and the way in which they bring about the fusion of the vesicle and plasma membranes remain pivotal unanswered questions in research into the molecular mechanism of Ca^{2+}-triggered exocytosis.

Many laboratories have approached this question by testing syt variants (mutants and isoforms) for function in secretion. However, the interpretation of such experiments depends on a full understanding of how each variant alters the various interactions. Charge neutralizing mutations of many of the residues that coordinate Ca^{2+} binding to syt I alter release in both synapses (Mackler *et al*., 2002; Stevens and Sullivan, 2003; Nishiki and Augustine, 2004) and neuroendocrine cells (Wang *et al*., 2006), but these mutations generally fail to show selectivity between the impairment of SNARE and PS binding. A mutation of a residue near a Ca^{2+}-coordinating aspartate of syt I reduced PS binding and synaptic transmission (Fernandez-Chacon *et al*., 2001), but this mutation also impaired Ca^{2+}-stimulated SNARE binding (Wang *et al*., 2003). Mutations in the linker connecting the C2A and C2B domains of syt I reduced SNARE binding and reduced exocytosis in neuroendocrine cells (Bai *et al*., 2004). Stopped-flow kinetic experiments and radiolabeled lipid binding measurements in this study indicated that the linker mutants failed to alter interactions with PS. However, more recent investigations in a lipid sedimentation assay showed that Ca^{2+}-dependent PS binding by the syt I linker mutants was impaired (Hui and Chapman, unpublished). Mutations of two different Ca^{2+}-binding aspartate residues in the C2A domain of syt I were initially reported to reduce PS binding but to have very small effects on synaptic transmission (Fernandez-Chacon *et al*., 2002). But these same

This article was published online ahead of print in *MBoC in Press* (http://www.molbiolcell.org/cgi/doi/10.1091/mbc.E10–04–0285) on June 23, 2010.

The online version of this article contains supplemental material at *MBC Online* (http://www.molbiolcell.org).

Address correspondence to: Meyer Jackson (MJackson@Physiology.Wisc.Edu).

Abbreviations used: PS, phosphatidylserine; SNARE, soluble N-ethylmaleimide sensitive factor receptor.

mutations were subsequently reported to have very different effects on lipid and SNARE binding and to alter synaptic transmission quite markedly (Pang *et al*., 2006). Mutations of residues in membrane penetrating loops of syt I have been found to enhance syt I-PS binding and synaptic transmission (Rhee *et al*., 2005), while a mutation in loop 2 of the C2A domain selectively reduced syt I-SNARE interactions (Martens *et al*., 2007; Lynch *et al*., 2008). Both classes of mutations altered exocytosis in PC12 cells, suggesting that both syt I-PS interactions and syt I-SNARE interactions play important roles in exocytosis (Lynch *et al*., 2008). However, the same loop penetrating mutations have since been reported to alter syt I-SNARE interactions as well (Hui *et al*., 2009). Thus, the precise roles of syt I-PS interactions and syt I-SNARE interactions in exocytosis remain unclear. Indeed, because syt I must bind PS in order to drive SNARE complex assembly, it may be impossible to resolve these two Ca^{2+}-triggered effector interactions using syt I mutations (Bhalla *et al*., 2006).

The syt protein family comprises 17 isoforms (Craxton, 2007), and functional comparisons between these isoforms offers another approach to elucidating the roles of Ca^{2+}-dependent interactions between syt I and its targets. Soluble C2 domains from various syt isoforms inhibited release from cracked PC12 cells, and this inhibition was correlated with t-SNARE binding activity (Tucker *et al*., 2003). The isoforms can be classified according to the kinetics of disassembly of syt from PS liposomes (Hui *et al*., 2005). Although syts with rapid, intermediate, and slow disassembly kinetics are capable of Ca^{2+}-induced membrane fusion in vitro (Bhalla *et al*., 2008), the kinetics of exocytosis mediated by members of these groups has yet to be evaluated.

Questions about the roles of these syt-effector interactions are further complicated by the fact that exocytosis can be resolved into a sequence of steps including vesicle docking, priming, fusion pore opening, and fusion pore dilation. Syt isoforms and mutations alter fusion pore lifetimes (Wang *et al*., 2001; Wang *et al*., 2003; Bai *et al*., 2004; Wang *et al*., 2006). Varying the expression of syt I and syt II alters the relative amounts of rapid and slow release (Nagy *et al*., 2006), and mutations of the lipid penetrating loops alter fusion pore dilation (Lynch *et al*., 2008). The fact that Ca^{2+} accelerates both fusion pore opening and fusion pore dilation raises the possibility that different syt I-effector interactions mediate distinct kinetic steps in exocytosis (Wang *et al*., 2006).

In the present study we have attempted to address the question of the roles of syt-effector interactions by evaluating both syt I mutants and syt isoforms. We utilized in vitro assays to test Ca^{2+}-stimulated PS binding, Ca^{2+}-stimulated (target-SNARE [t-SNARE]) binding, and Ca^{2+}-stimulated t-SNARE assembly of two syt I mutants (R399A and T328A, Figure 1A), selected to produce very different alterations in these interactions (Gaffaney *et al*., 2008). We also evaluated syt isoforms with widely divergent interactions. Using amperometry to measure norepinephrine release and to resolve distinct kinetic steps of exocytosis (Chow and von Rüden, 1995; Travis and Wightman, 1998), we found that PC12 cells overexpressing these syt variants showed alterations in the overall rate of exocytosis, as well as fusion pore stability. In agreement with previous work on cells with different PS levels (Zhang *et al*., 2009), our results suggest that Ca^{2+}-triggered PS binding has multiple functions in exocytosis, including a stabilization of open fusion pores by retarding the rate of fusion pore dilation. By contrast, variations in Ca^{2+}-triggered SNARE binding and assembly do not appear to be correlated with the steps of exocytosis tested here.

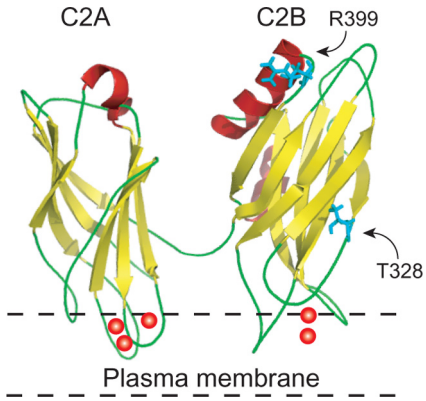

Figure 1. Protein backbone structure of the cytoplasmic domain of syt I C2AB in ribbon format, with the membrane sketched below. The solution structures of C2A and C2B were modified from (Shao *et al*., 1998) and (Fernandez *et al*., 2001). Red spheres depict bound Ca^{2+}. The residues mutated for this study, R399 and T328, are indicated and their side chains are rendered in blue.

MATERIALS AND METHODS

Plasmid Construction, Cell Culture, and Transient Transfection

Full length syt I, syt VII, and syt IX were cloned into the pIRES2-EGFP vector. Syt I(T328A) and syt I(R399A) were generated using the QuikChange site-directed mutagenesis kit (Stratagene, Santa Clara, CA). All constructs were verified by sequencing. Syt I C2AB, C2AB T328A, C2AB R399A, syt VII C2AB, syt IX C2AB, full-length syntaxin, and SNAP-25 were expressed in pTrcHisA vector (Bhalla *et al*., 2006; Bhalla *et al*., 2008; Gaffaney *et al*., 2008). For coflotation and cosedimentation experiments, syt I C2AB, syt VII C2AB, and syt IX C2AB were expressed using pGEX-2T. Plasmids encoding SNAP-25 and syntaxin 1a (used to make heterodimers) were kindly provided by J.E. Rothman (Columbia University).

PC12 cells were cultured in an incubator at 37°C with 10% CO_2 and transfected using an electroporator upon reaching ~90% confluence (ECM 830; BTX, Hawthorne, NY). Cells were split into 35-mm dishes coated with collagen I (BD Biosciences, San Jose, CA) and poly-D-lysine (Sigma) and loaded with 1.5 mM norepinephrine and 0.5 mM ascorbate 14–16 h before experiments. Amperometry was performed 48–96 h after transfection.

Protein Expression and Purification

For His-tagged syt I C2AB, C2AB T328A, C2AB R399A, syt VII C2AB, syt IX C2AB, and SNAP25, *Escherichia coli* were grown at 37°C to an OD_{600} of 0.8 and protein expression was induced with 0.4 mM IPTG. Four hours after induction the bacteria were collected by centrifugation and the pellet was resuspended in His6 buffer (25 mM HEPES-KOH, 500 mM NaCl, 20 mM imidazole). Resuspended bacteria were subjected to sonication (2 × 45 s; 50% duty cycle). Triton X-100 (2%) and protease inhibitors (1 μg/ml aprotinin, pepstatin, and leupeptin; 0.5 mM PMSF) were added to the sonicated material and incubated for 2–3 h with rotation at 4°C. Samples were centrifuged to remove insoluble material. The supernatant was incubated with Ni^{2+}-Sepharose HP beads overnight. The following day, the Ni^{2+} beads were washed twice with His6 wash buffer containing 25 mM HEPES, 1M NaCl, 1 mM $MgCl_2$, 20 mM imidazole, 0.1 mg/ml RNase and DNase, followed by two more washes with His6 buffer. Beads were collected and eluted with 1.5 volumes of elution buffer (25 mM HEPES-KOH, 400 mM KCl, 500 mM imidazole, 5 mM 2-mercaptoethanol). Eluted protein was dialyzed against solution containing 25 mM HEPES-KOH, 250 mM KCl, 10% glycerol, and 0.16 g/L dithiothreitol (DTT).

For His-tagged t-SNARE heterodimers and full-length syntaxin, *E. coli* were grown and collected as described above. The pellet was resuspended in resuspension buffer (25 mM HEPES-KOH, 400 mM KCl, 20 mM imidazole, and 5 mM 2-mercaptoethanol). Resuspended bacteria were subjected to sonication and treated with Triton X-100 (2%), protease inhibitors, RNase, and DNase. Insoluble material was removed by centrifugation, and the supernatant was applied to a Ni^{2+} column using AktaFPLC (GE-Amersham Biosciences, Piscataway, NJ). The column was washed extensively with resuspension buffer containing 1% Triton X-100 and then *n*-octylglucoside wash buffer (25 mM HEPES-KOH, 400 mM KCl, 50 mM imidazole, 10% glycerol, 5 mM 2-mercaptoethanol, 1% *n*-octylglucoside). The bound protein was eluted using *n*-octylglucoside wash buffer with 500 mM imidazole.

The procedure for purification of GST (glutathione-S-transferase)-tagged C2AB domains of syt I, VII, and IX was similar to that of His-tagged proteins.

In brief, bacteria pellets were resuspended in HEPES-buffered saline (HBS) buffer (25 mM HEPES, 100 mM NaCl, pH 7.4) followed by sonication and treatment with Triton X-100 and protease inhibitors. After centrifugation, the supernatant was incubated with glutathione sepharose beads (GE Healthcare, Piscataway, NJ) overnight at 4°C. Beads were washed twice with wash buffer followed by two washes with HBS buffer. The GST tag was removed by thrombin cleavage. PMSF was added to inactivate the thrombin.

All proteins were subjected to SDS-PAGE and stained with Coomassie blue to determine concentration against a BSA standard curve.

Protein Reconstitution (t-SNAREs)

Liposomes with t-SNAREs were prepared as described previously (Tucker *et al.*, 2004). Briefly, palmitolyoleoylphosphatidylcholine (POPC) (Avanti Polar Lipids, Alabastar, AL) in chloroform was dried under a stream of nitrogen and subjected to vacuum for >1 h. The syntaxin·SNAP-25 complex was diluted to 0.8 mg/ml. The dried lipid was suspended in the syntaxin·SNAP-25 mixture, diluted with reconstitution buffer (25 mM HEPES-KOH, 100 mM KCl, 10% glycerol, 1 mM DTT), and dialyzed against reconstitution buffer overnight. The dialyzed vesicles were collected, mixed with 80% Accudenz, and transferred into ultra clear centrifuge tubes. A step gradient was prepared by the addition of 30 and 0% Accudenz layers onto the vesicle layer. The samples were centrifuged at 55,000 rpm for 1 h 45 min (SW-55 rotor). Vesicles were collected from the 0/30% interface and analyzed by SDS-PAGE to verify protein incorporation. To make liposomes bearing full-length syntaxin (for the assembly assay), the composition of liposomes was 15% palmitoyloleoylphosphatidylserine (POPS), 55% POPC, and 30% palmitoyloleoylphosphatidylethanolamine.

Cosedimentation Assay

Chloroform solutions of POPC and POPS (Avanti Polar Lipids) were mixed as indicated, dried under nitrogen, further dried by vacuum, and resuspended in HBS buffer. The suspension was passed through a polycarbonate filter to generate 252 nm liposomes (Hui *et al.*, 2009). Protein (0.35 nmoles) was incubated with designated concentration of liposomes in the presence of 1 mM Ca^{2+} or 0.2 mM EGTA for 15 min at 22°C. This mixture was centrifuged at 65,000*g* for 40 min at 4°C. Supernatant was subjected to SDS/PAGE and analyzed by Image J after Coomassie blue staining. Bound protein was expressed as a percentage of the total input. Liposome concentration was calculated from lipid concentration by scaling the estimate to that for 100 nm liposomes. Scaling the relation 1 mM lipid = 11 nM liposome (Bai *et al.*, 2004) to 252 nm liposomes, we obtain 1 mM lipid = 11 × ($100^2/252^2$) nM liposome = 1.73 nM liposome.

Coflotation and Assembly Assays

For the coflotation assay, reaction mixture was prepared containing 10 μM C2AB (syt mutations or isoforms), 45 μl t-SNARE heterodimer bearing liposomes, and reconstitution buffer in the presence of 1 mM Ca^{2+} or 0.2 mM EGTA. Reaction mixture (100 μl) was incubated at room temperature for 30 min with shaking. Following incubation, the vesicles were mixed with 100 μl of 80% Accudenz (with or without Ca^{2+}), transferred to ultra clear centrifuge tubes, and overlaid with 35%, 30%, and 0% Accudenz (with or without Ca^{2+}) to form a step gradient. Gradients were centrifuged at 55,000 rpm for 1 h 45 min (SW-55 rotor), and 40 μl of vesicles was collected from the 0/30% interface and analyzed by SDS-PAGE and Coomassie blue staining. For the assembly assay, full-length syntaxin bearing liposomes replaced t-SNARE heterodimer bearing liposomes and 10 μM SNAP-25 was added.

Amperometry

Norepinephrine release was recorded with a VA-10 amperometry amplifier (ALA Scientific, Farmingdale, NY) using 5-μm carbon fiber electrodes held at 650 mV (Zhang and Jackson, 2008). Cells were bathed in a solution containing 150 mM NaCl, 4.2 mM KCl, 1 mM NaH_2PO_4, 0.7 mM $MgCl_2$, 2 mM $CaCl_2$, and 10 mM HEPES (pH 7.4). Secretion was evoked by pressure application of a solution identical to bathing solution but with 105 mM KCl and 5 mM NaCl.

Western Blots

PC12 cells were harvested in PBS with 1% Triton X-100 and 5 mM PMSF. Samples were incubated at 4°C for 30 min and then centrifuged at 21,000*g* for 10 min. Supernatants were transferred to new tubes, and protein concentration was determined using the BCA protein assay kit (Pierce Chemical, Rockford, IL). Ten micrograms of protein extract was subjected to SDS-PAGE. Proteins were detected with monoclonal antibodies against synaptotagmin I (Cl 41.1), synaptotagmin VII (this laboratory), synaptotagmin IX (this labora-

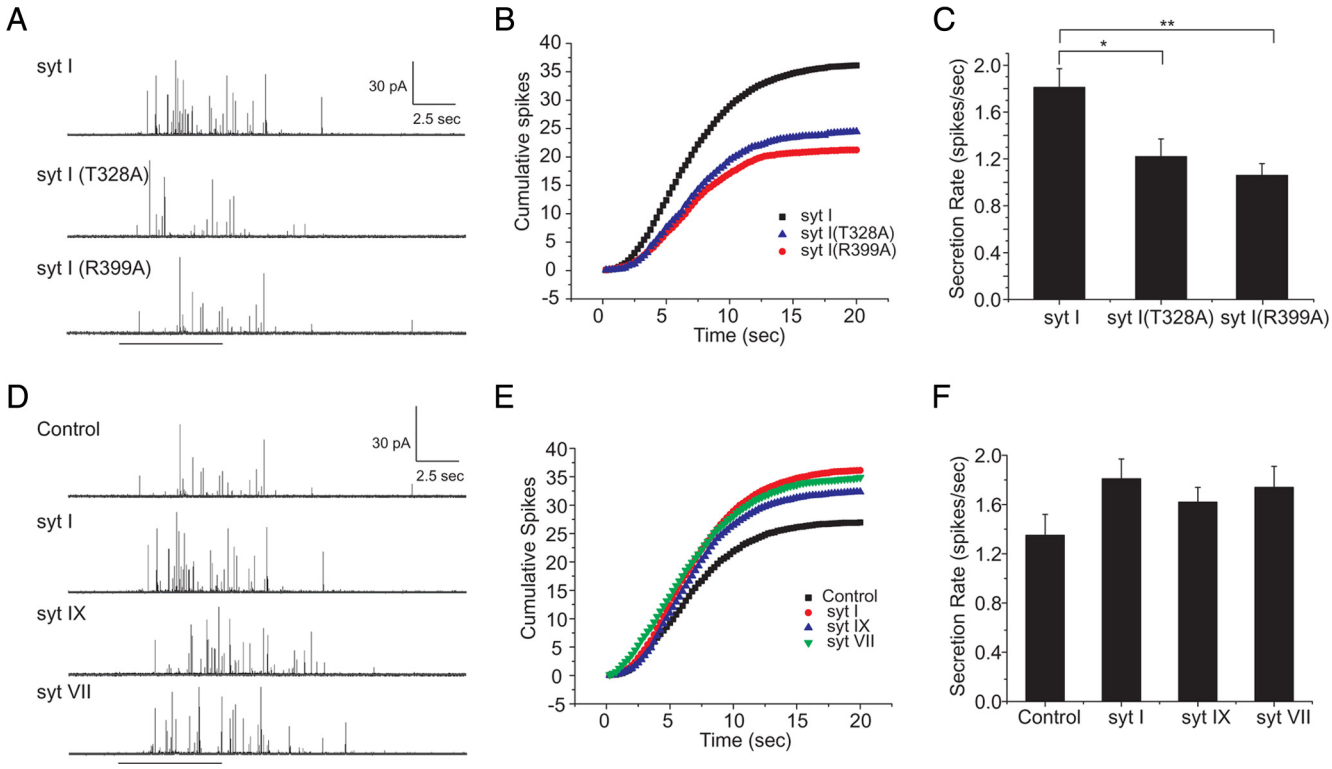

Figure 2. Syt I mutations and isoforms affect secretion rate. (A) Sample amperometry traces for wild-type syt I and two syt I mutants. The thick horizontal line below indicates the time of depolarization by a puff of high KCl. (B) Cumulative spike counts were plotted versus time to illustrate the time course of fusion triggered by depolarization (starting at t = 0). (C) Secretion rates for the different mutants were computed as number of spikes in the first 20 s. Amperometry traces for different syt isoforms (D), cumulative spike plots (E), and secretion rates (F). Data were from 42 to 125 cells. *, $p < 0.05$; **, $p < 0.01$. Error bars represent SEM.

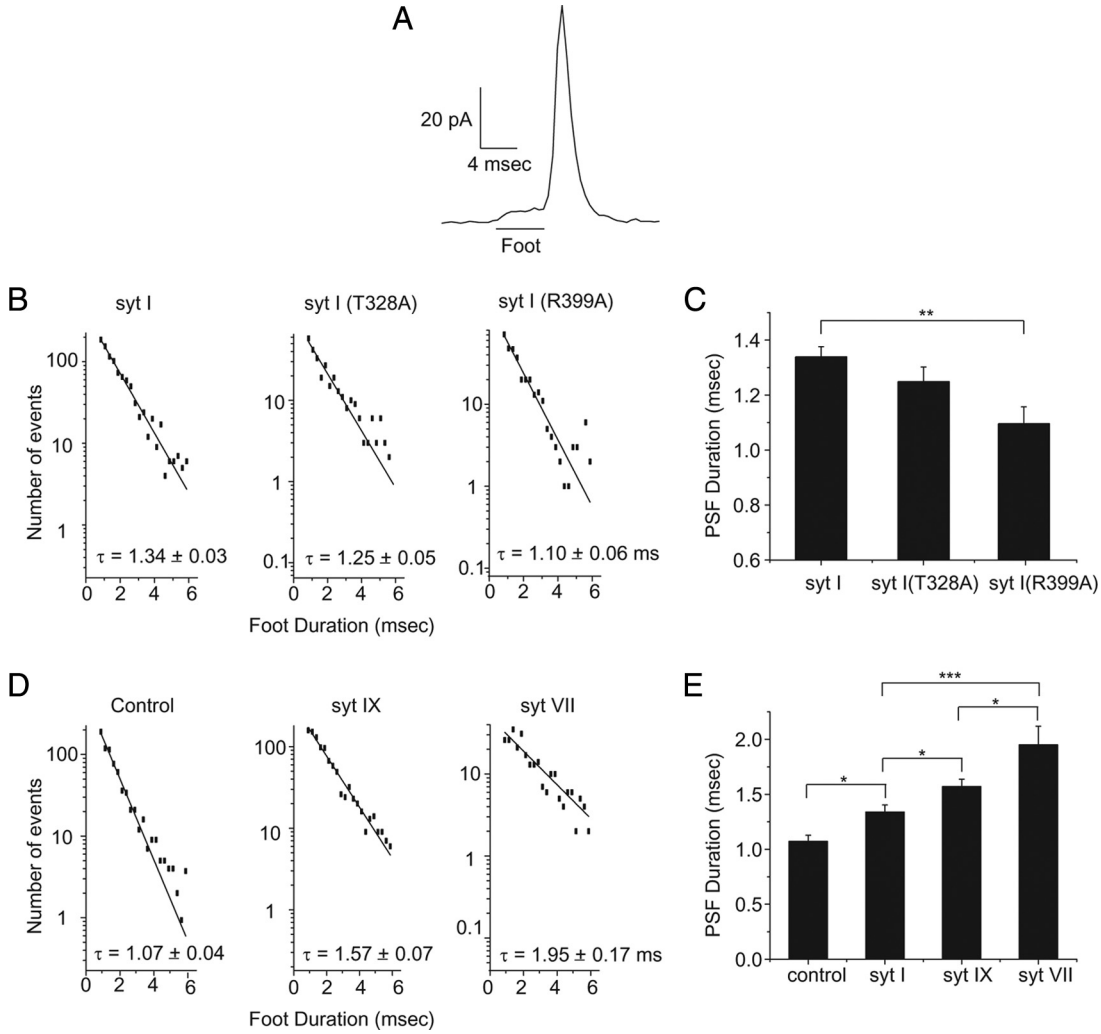

Figure 3. Syt I mutations and isoforms affect fusion pore stability. (A) Sample trace with an expanded view of a single vesicle release event showing the prespike foot (PSF). (B) Fusion pore lifetime distributions for wild-type syt I and two mutants, and (C) their mean fusion pore lifetimes. (D) Fusion pore lifetime distributions for control, syt VII, and syt IX (for syt I see B), and (E) their mean fusion pore lifetimes. 315-1021 prespike feet from 42 to 125 cells. *, $p < 0.05$; **, $p < 0.01$; ***, $p < 0.001$. Error bars represent SEM.

tory), syntaxin (HPC-1), SNAP-25 (Cl 71.1), and VAMP (Cl 69.1), followed by secondary horse radish peroxidase conjugated antibody, and developed with enhanced chemiluminescence (Pierce).

Data Analysis

Secretion rate and amperometry spikes were analyzed as described previously (Zhang and Jackson, 2008). Spikes with peak amplitudes ≥2 pA were counted in the determination of secretion rate. Cells with extremely low (<3) or high (>100) spike numbers during 20 s for a single application of KCl solution were excluded. Fusion pore lifetimes were taken as the duration of prespike feet (PSF) measured for spikes with amplitudes ≥20 pA (see Figure 3A). Kiss-and-run events arising from fusion pores that also give rise to PSF were recognized as rectangular events with peak amplitudes between 2 and 3.5 pA (Wang *et al*., 2006) (see Figure 4A). The Student's *t* test was used to evaluate statistical significance. One-way ANOVA and Dunnett's test were also applied to evaluate statistical significance, and the results were very similar to the *t* test. Numbers of cells and events analyzed are presented in the figure legends. For evaluation of statistical significance in event frequency measurements we used the number of cells per recordings as the number of measurements; for fusion pore kinetics we have previously shown that there is no dependence on cells per recordings, so the number of PSF was used (Wang *et al*., 2006).

RESULTS

Amperometry recording monitored the release of norepinephrine from PC12 cells and revealed single vesicle release events with high temporal resolution. The exocytosis of a vesicle often begins with the opening of a fusion pore, producing a low flux of norepinephrine that generates an amperometric current of ~2 pA (see Figure 3A). When a fusion pore starts to dilate the norepinephrine flux rises sharply, producing a spike as the bulk of the remaining vesicle content escapes. In some instances a fusion pore closes without dilating to produce a kiss-and-run event (see Figure 4A). In the present study we analyzed the frequency of fusion events as a measure of the overall secretion rate. Events are seen if a pore opens, so this frequency reflects relatively early kinetic processes up to the actual opening of fusion pores. PSF and kiss-and-run events were analyzed to investigate fusion pore dynamics. This gives us insight into kinetic steps taken by an open fusion pore, and focuses on a later kinetic phase in exocytosis compared with the early steps that influence event frequency.

Our studies focused on two syt I mutations (T328A and R399A) and three syt isoforms (syt I, syt VII, and syt IX). The mutants were selected because of their contrasting effects on syt-PS and syt-SNARE interactions. Syt I and syt IX are the major isoforms in PC12 cells but traces of syt IV and syt VII

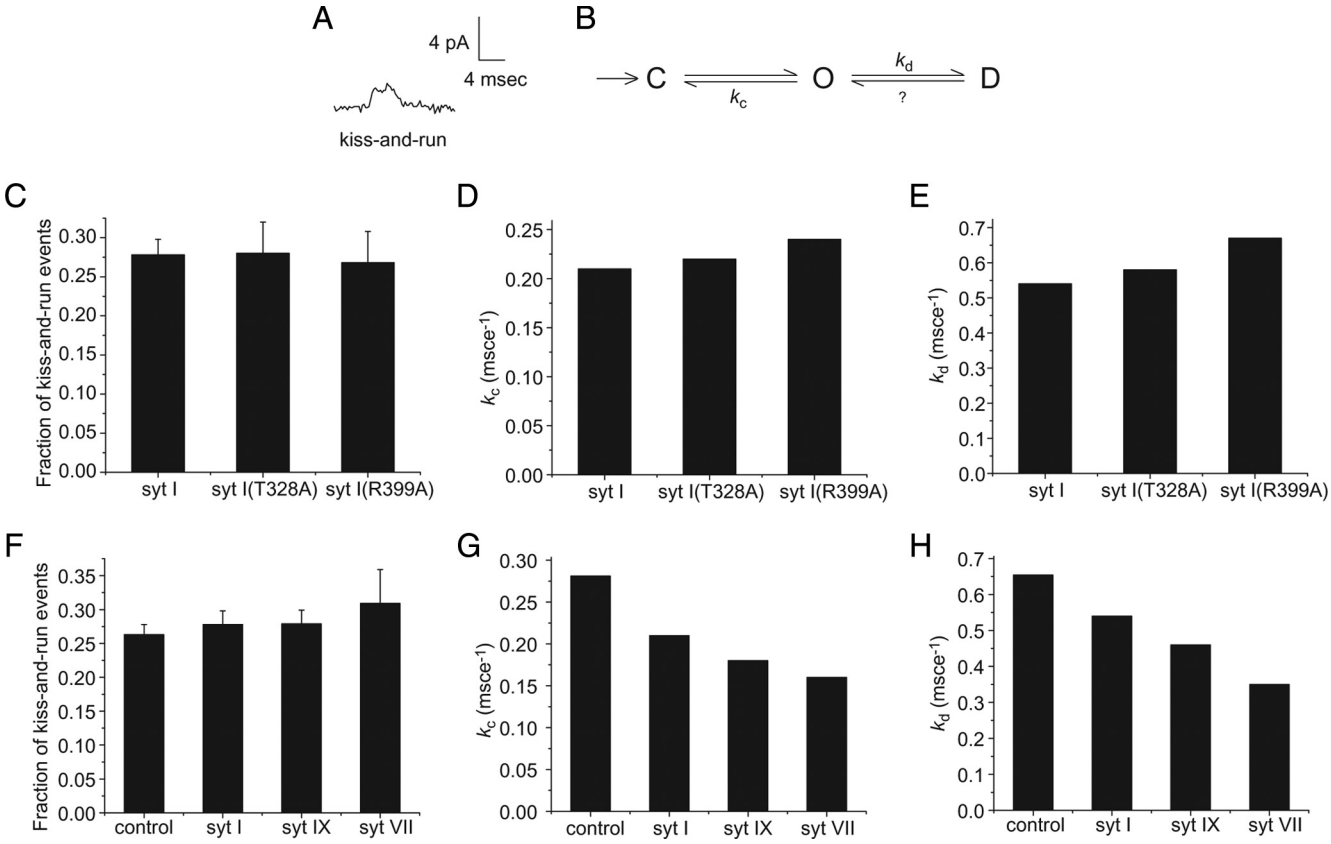

Figure 4. The effect of syt I mutations and isoforms on fusion pore dynamics. (A) A sample amperometry recording of a kiss-and-run event. (B) The model of fusion pore kinetics used to determine the rate constants k_c and k_d from mean fusion pore lifetime and fraction of kiss-and-run events (Wang *et al*., 2006). (C) Fraction of kiss-and-run events. (D and E) Computed values of k_c, and k_d for wild-type syt I and two mutants. (F) Fraction of kiss-and-run events. (G and H) Computed values of k_c, and k_d for syt isoforms. Same data sets as Figure 3.

can also be detected (Tucker *et al*., 2003; Ahras *et al*., 2006; Zhang *et al*., 2010). Western blots indicate that overexpressing these isoforms and mutants elevates the levels in culture by ~threefold (Supplemental Figure 1). Because ~30% of the cells in culture are transfected (as judged by GFP fluorescence), the cells we record from have levels ~10-fold higher than the respective native protein. Furthermore, these Western blots showed that overexpression of these syt variants had no effect on the levels of other syt isoforms or the levels of syntaxin 1a, syntaxin 1b, SNAP-25, or synaptobrevin/VAMP. Immuno-gold labeling has shown that overexpressed syt VII (Fukuda *et al*., 2004) and syt IX correctly target to dense-core vesicles (Zhang, Chapman, and Jackson, in preparation). These experiments provide some assurance that the effects of the syt variants studied here result from direct functions within the exocytotic apparatus.

Exocytosis and Fusion Pore Regulation by Syt Mutations and Isoforms

Syt I(R399A), with its mutation on the surface of the C2B domain opposite of the lipid-penetrating loops (Figure 1), does not stimulate SNARE-mediated Ca^{2+}-triggered liposome fusion as effectively as wild-type syt I, but its binding to t-SNAREs is comparable to wild type (Gaffaney *et al*., 2008). We found that overexpression of syt I(R399A) in PC12 cells reduced the secretion rate by 41% (Figure 2, A–C; 1.06 ± 0.10 spikes/s versus the rate of 1.81 ± 0.16 spikes/s in cells overexpressing wild-type syt I; $p < 0.01$) and decreased the PSF lifetime by 18% (Figure 3, B and C; 1.10 ± 0.06 msec versus 1.34 ± 0.06 with wild-type syt I; $p < 0.01$). Syt I(T328A) provides a contrast to syt I(R399A). Its mutation resides on the side of the C2B domain close to the lipid-penetrating loops (Figure 1). Syt I(T328A) binds t-SNAREs more strongly than wild-type syt I but fails to promote liposome fusion as efficiently as wild-type syt I (Gaffaney *et al*., 2008). Overexpression of syt I(T328A) in PC12 cells reduced the secretion rate by 33% (Figure 2, A–C; 1.22 ± 0.15 spikes/s, $p < 0.05$) but left the fusion pore lifetime unaltered (Figure 3, B and C, 1.25 ± 0.05 msec, $p > 0.05$).

To analyze the fusion pore properties of these two syt I mutants in greater detail we focused on kiss-and-run events (Figure 4A), which are indicative of a return of an open pore to the preceding closed state, rather than dilation (Figure 4B). The fraction of such events failed to change significantly when mutants of syt I were expressed (Figure 4C). Using this fraction together with the mean fusion pore lifetime enabled us to determine the rate constants for transitions of the open fusion pore to the dilating state (k_d) and return transitions to the closed state (k_c) (Figure 4B). Both syt I(R399A) and (T328A) increased both of these rate constants, but R399A had greater effects (Figure 4, D and E). The larger increases with R399A suggest that the decrease in fusion pore lifetime resulting from this mutation reflects both more rapid fusion pore dilation and more rapid fusion pore closure.

Overexpression of syt I, syt VII, or syt IX produced similar small increases in the secretion rate that were similar in magnitude, indistinguishable from one another (Figure 2, D–F; $p > 0.05$) and statistically indistinguishable from con-

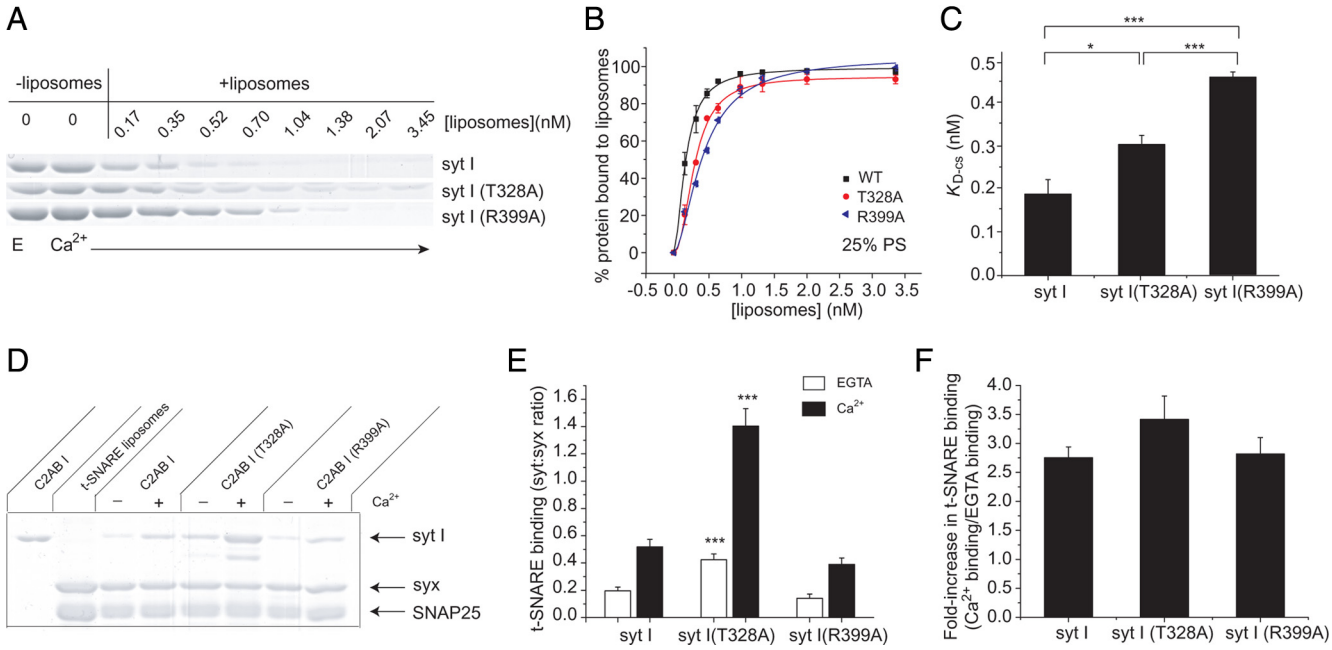

Figure 5. PS and t-SNARE binding properties of syt I mutations. (A) A sample cosedimentation gel for syt I mutants bound to the indicated concentrations of liposomes (containing 25% PS). [Ca^{2+}] = 1 mM. (B) Percentage of protein bound to liposomes plotted versus liposome concentration. (C) K_D-cs values for syt mutations derived from plots in B. (D) A sample cofloatation gel for syt-t-SNARE binding. (E) Syt-t-SNARE binding in the presence of Ca^{2+} or EGTA. (F) Fold-increase in t-SNARE binding (binding in Ca^{2+}/binding in EGTA) computed as the ratio from the values in E. Data from at least three independent experiments. *, $p < 0.05$; ***, $p < 0.001$. Error bars represent SEM.

trol cells overexpressing blank vector (Figure 2, D–F; $p > 0.05$). Overexpression of syt I, syt VII, and syt IX all prolonged fusion pore lifetime, with syt VII exhibiting the strongest effect (Figure 3, C and D). The increase produced by syt I confirms a previous result (Wang *et al.*, 2001). These syt isoforms did not change the fraction of kiss-and-run events (Figure 4F) but decreased k_c and k_d (Figure 4, G and H). Thus, both the increase in fusion pore stability seen with isoform overexpression as well as the decrease seen with the syt I(R399A) arise from changes in both of the fusion pore exit rates.

Syt-PS and Syt-t-SNARE Interactions

Many syts bind to PS-containing lipid bilayers and to SNARE proteins in a Ca^{2+}-dependent manner (Brunger, 2005; Chapman, 2008). We therefore examined these interactions in the syt mutants and isoforms investigated above with the goal of relating changes in exocytotic function to changes in in vitro interactions. Our cosedimentation measurements with PS-containing liposomes showed that syt I(R399A) had impaired lipid binding, while coflotation measurements confirmed that its t-SNARE interaction was indistinguishable from wild type (Gaffaney *et al.*, 2008) (Figure 5). Thus, the decreases in secretion rate and PSF lifetime seen with this mutant suggest that impairing syt-PS binding reduces the rate of fusion and destabilizes open fusion pores (Figures 2, A–C and 3, B and C). Syt I(T328A) had reduced PS binding activity, but t-SNARE binding increased, both in the presence and absence of Ca^{2+} (Figure 5). Thus, the T328A mutation has opposite effects on PS binding and t-SNARE binding. We note that the t-SNARE binding in EGTA evident in Figures 5E and 6E confirms earlier studies demonstrating a Ca^{2+}-independent interaction between syntaxin and synaptotagmin (Bennett *et al.*, 1992; Gaffaney *et al.*, 2008). Here, we will evaluate the functional significance of both of these interactions in parallel.

Syt isoforms vary in their binding to PS and SNARE proteins (Tucker *et al.*, 2003; Bhalla *et al.*, 2008). Cosedimentation experiments showed that syt VII bound to PS the most tightly, with syt IX second, and syt I third (Figure 6, A–C). Coflotation experiments showed that syt VII had the strongest t-SNARE binding activity, either in the presence of Ca^{2+} or in the presence of EGTA, but the increases in t-SNARE binding in Ca^{2+} (binding in Ca^{2+}/binding in EGTA) were weaker than for syt I or syt IX (Figure 6, D–F). (Note that soluble C2AB domain of each isoform was purified as a GST fusion protein with the GST-tag removed by thrombin. The mutants were purified with his-tags. This difference influences the binding properties and is responsible for the differences between the syt I data in figures presenting isoform results versus mutant results, e.g., Figures 5, E and F and 6, E and F).

Syt also regulates the Ca^{2+}-dependent assembly of t-SNAREs (Bhalla *et al.*, 2006), so we conducted assembly measurements with the syt isoforms and mutants of this study. These experiments were performed with syntaxin-bearing liposomes; we determined the recruitment SNAP-25 that was stimulated by syt in the presence and absence of Ca^{2+} (Figure 7). Both syt I mutants (Figure 7B) and syt isoforms (Figure 7C) differed in their capacity to drive the association of SNAP-25 with syntaxin in response to Ca^{2+}. Syt I (R399A) reduced assembly compared with wild type and syt I (T328A) (Figure 7B). Syt IX was the most effective isoform in promoting assembly, and syt I was the least effective (Figure 7C). To insure that SNAP-25 was assembled with syntaxin and not recruited by syt, EGTA was added to remove excess syt following the Ca^{2+} assembly step (± lanes of Figure 7A). The EGTA reduced syt but not the SNAP-25.

Evaluation of in Vitro Interactions in Exocytosis

To evaluate the binding results in terms of functional roles, the secretion rate and fusion pore lifetime were plotted versus various measurements of syt-effector interactions.

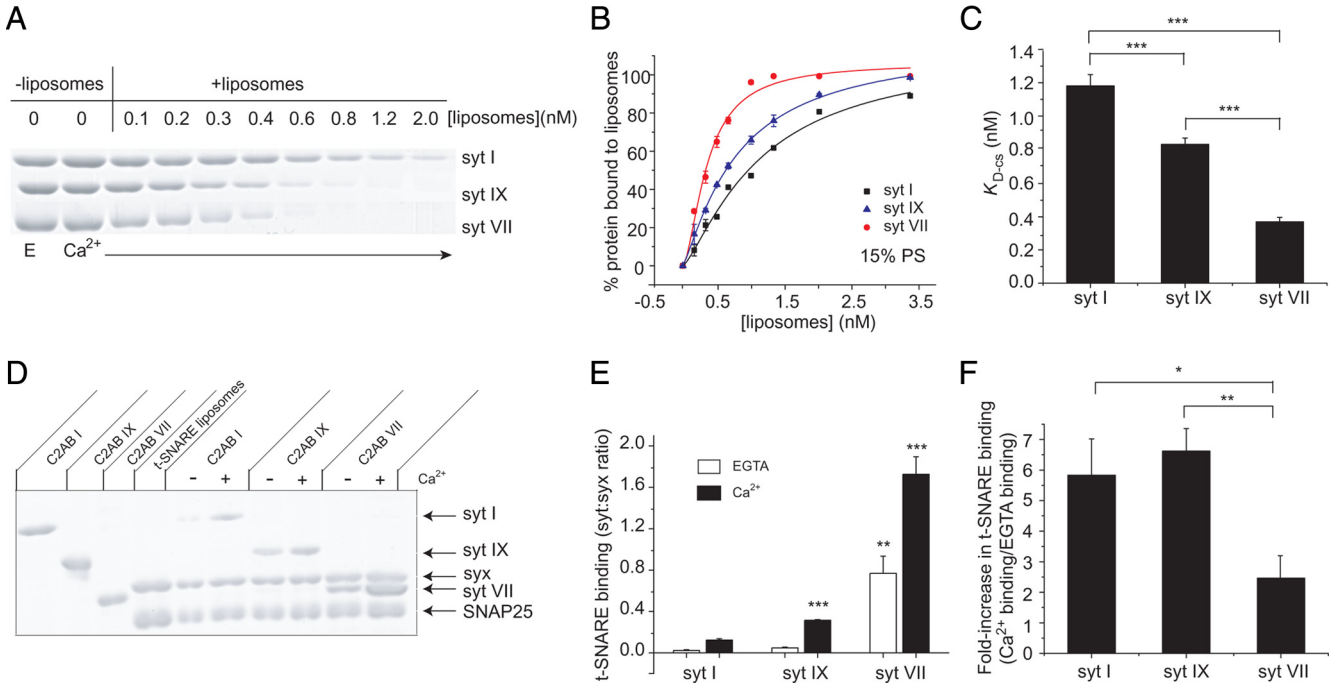

Figure 6. PS binding and t-SNARE binding by syt isoforms. (A) A sample cosedimentation gel for syt isoforms bound to the indicated concentrations of liposomes (containing 15% PS). [Ca^{2+}] = 1 mM. (B) Percentage of protein bound to liposomes plotted versus liposome concentration. (C) K_D-cs values for syt mutants derived from plots in B. (D) A sample cofloatation gel for syt-t-SNARE binding. (E) Syt-t-SNARE binding in the presence of Ca^{2+} or EGTA. (F) Fold-increase in t-SNARE binding (binding in Ca^{2+}/binding in EGTA) computed as the ratio from the values in E. Data from at least 3 independent experiments. *, $p < 0.05$; **, $p < 0.01$; ***, $p < 0.001$. Error bars represent SEM.

For mutants, these plots showed that the secretion rate decreased slightly with increases in the dissociation constant for syt-PS binding (K_D-cs), but this change was not statistically significant (Figure 8, A and D; $p = 0.20$). In plots of fusion pore lifetime versus K_D-cs we observed a significant decline with a slope of −0.89 (Figure 8D; $p = 0.03$). Plots of secretion rate and fusion pore lifetime versus syt-t-SNARE interactions in the presence of EGTA or Ca^{2+}, as well as the

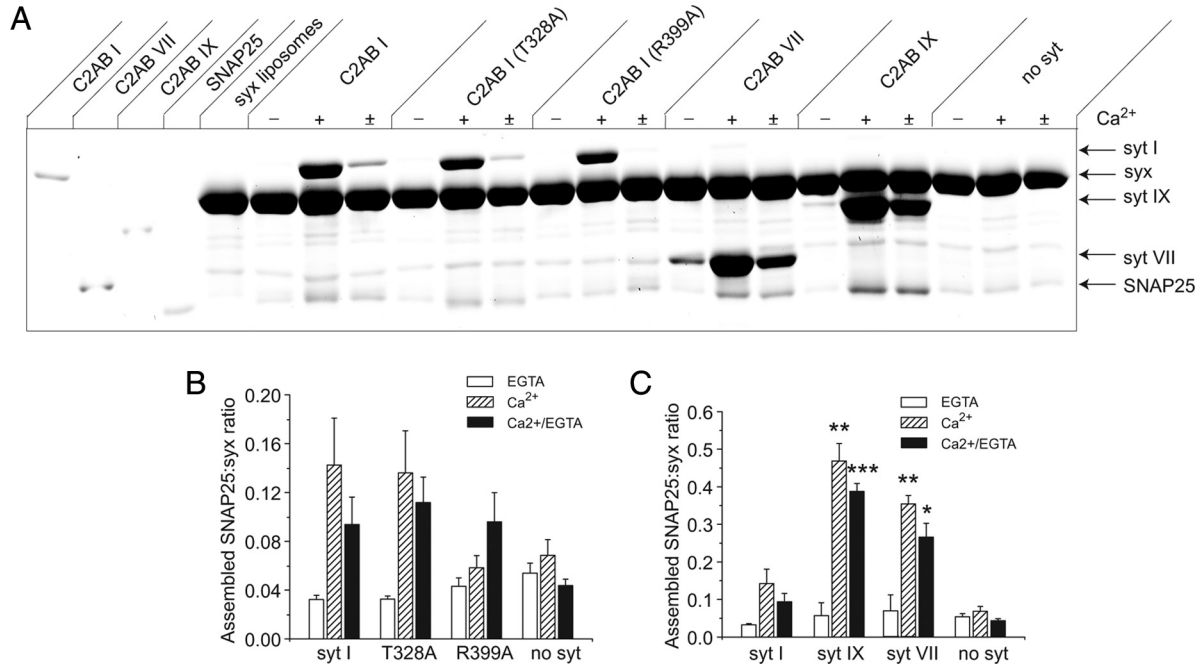

Figure 7. Syt mutants and isoforms regulate t-SNARE assembly. (A) Samples were incubated in 1 mM Ca^{2+} or 0.2 mM EGTA for 1 h as indicated by + and −. ± represents the addition of 2 mM EGTA for another 30 min following incubation in 1 mM Ca^{2+} before the coflotation experiment. The intensity ratios for SNAP-25 and syntaxin were averaged for mutants (B) and isoforms (C). Data were pooled from at least 3 independent experiments. *, $p < 0.05$, **, $p < 0.01$; ***, $p < 0.001$. Error bars represent SEM.

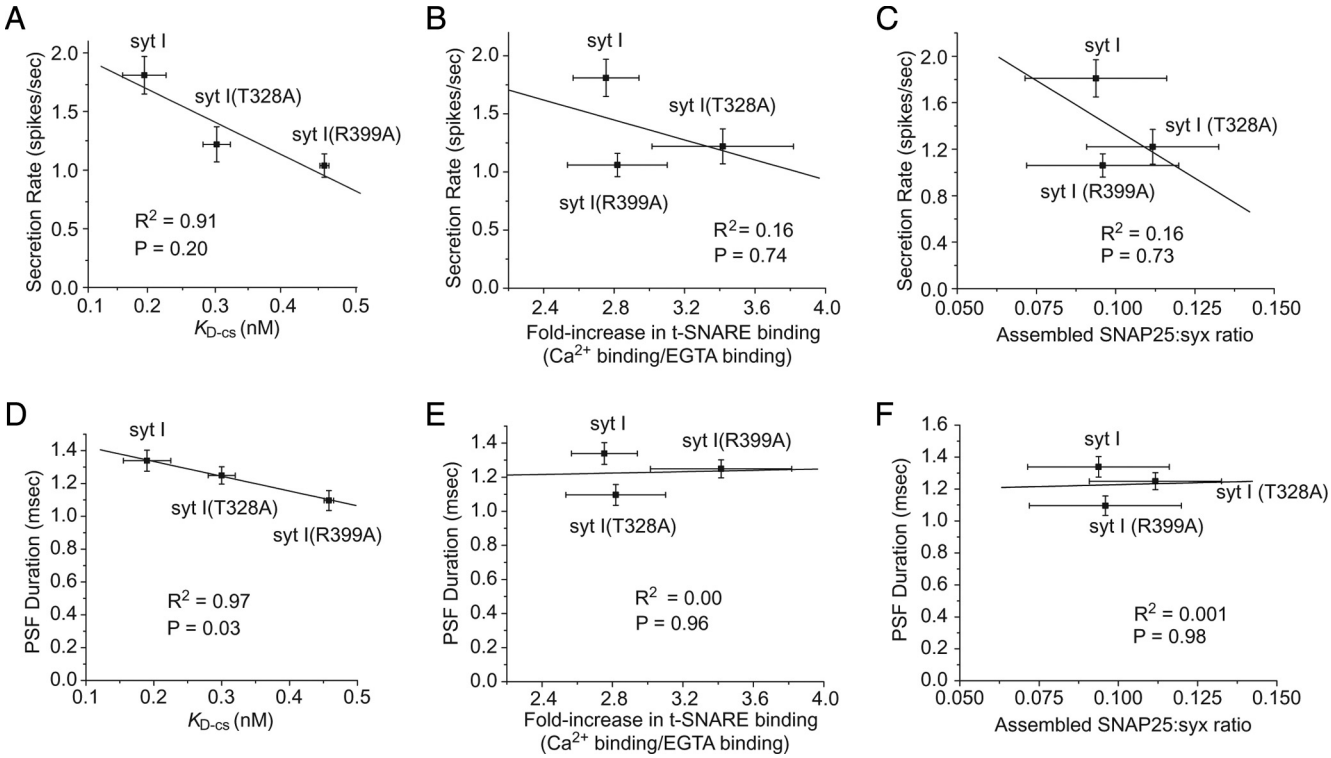

Figure 8. Test for correlation between in vitro interactions and exocytosis in syt I mutants. Plots of secretion rate versus PS-liposome binding *K*D-cs (A), fold-increase in t-SNARE binding (Ca^{2+} binding/EGTA binding) (B), and syt-induced t-SNARE assembly (C). Plots of PSF lifetime versus *K*D-cs (D), fold-increase in t-SNARE binding (binding in Ca^{2+}/binding in EGTA) (E), and syt-induced t-SNARE assembly (F). A statistically significant correlation was found only for PSF duration versus *K*D-cs (D).

fold increase in SNARE binding (binding in Ca^{2+}/binding in EGTA), exhibited no correlations (Figure 8, B and E, and Supplemental Figure 2), supporting the idea that syt-PS interactions play a more important role than either Ca^{2+}-dependent or Ca^{2+}-independent syt-t-SNARE interactions. The results shown in Figure 8 suggest that alterations in the strength of the syt-PS interaction dominate over alterations in the strength of the syt-t-SNARE interaction in the regulation of secretion and fusion pore stability.

For isoforms, plots of secretion rate versus *K*D-cs (Figure 9A), fold increase in SNARE binding (*K*D-cs in Ca^{2+}/*K*D-cs in EGTA, Figure 9B), and of the Ca^{2+}-dependent and independent t-SNARE interaction (Supplemental Figure 3) yielded no statistically significant correlation. The plot of fusion pore lifetime versus *K*D-cs showed a significant correlation (Figure 9D) with a slope of -0.76 ($p = 0.04$). Plots of fusion pore lifetime versus fold increase in SNARE binding (binding in Ca^{2+}/binding in EGTA) showed no correlation (Figure 9E, $p = 0.81$). The finding that isoforms alter fusion pore stability but not the overall secretion rate suggests that the regulation of fusion pores is distinct from the regulation of secretion rate, a conclusion reached previously based on the distinct Ca^{2+} dependences of these two processes (Wang *et al*., 2006).

In plots of secretion rate and PSF lifetime versus t-SNARE assembly triggered by Ca^{2+}-syt, we saw no correlation either for mutants (Figure 8, C and F) or for isoforms (Figure 9, C and F). These results failed to reveal a role for syt-induced SNARE assembly in either of these two phases of Ca^{2+}-triggered exocytosis. Parameters related to spike shape showed no correlation with the syt-PS or syt-t-SNARE interactions, either for the syt mutants (Supplemental Figure 4) or syt I isoforms (Supplemental Figure 5). These results are in keeping with the notion that spike shape reflects the kinetics of diffusion of vesicle content through an expanding pore rather than structural rearrangements of protein and lipid within the membrane (Zhang and Jackson, 2008).

Because syt-PS binding showed a correlation with fusion pore lifetime, we looked more closely at fusion pore transitions. The fraction of kiss-and-run events showed a weak and insignificant correlation with *K*D-cs for syt mutants (slope = -0.04; $p = 0.37$, Figure 10A) and isoforms (slope = -0.04; $p = 0.26$, Figure 10D). k_c and k_d increased in parallel with *K*D-cs with respective slopes of 0.11 and 0.49 for syt mutations (Figure 10B, $p = 0.06$; Figure 10C, $p = 0.08$) and 0.06 and 0.23 for syt isoforms (Figure 10E, $p = 0.12$; Figure 10F, $p < 0.01$). These results support the hypothesis that the syt-PS interaction impedes both fusion pore dilation and closure. The slopes of plots of k_d versus *K*D-cs were ~4 times larger than those from plots of k_c versus *K*D-cs, indicating that the syt-PS interaction stabilizes open fusion pores primarily by inhibiting the transition of open fusion pores to the dilating state.

DISCUSSION

We have used amperometry to evaluate the influence of syt I mutations and syt isoforms on distinct kinetic phases in the release of norepinephrine from PC12 cells. This study has shown that overexpression of syt I mutants reduced the overall rate of fusion in PC12 cells. These syt I mutants as well as the syt isoforms, syt I, syt VII, and syt IX, altered the rates of fusion pore transitions. These studies confirm the capacity of syt to influence fusion pores (Wang *et al*., 2001; Wang *et al*., 2003; Bai *et al*., 2004; Wang *et al*., 2006), extending

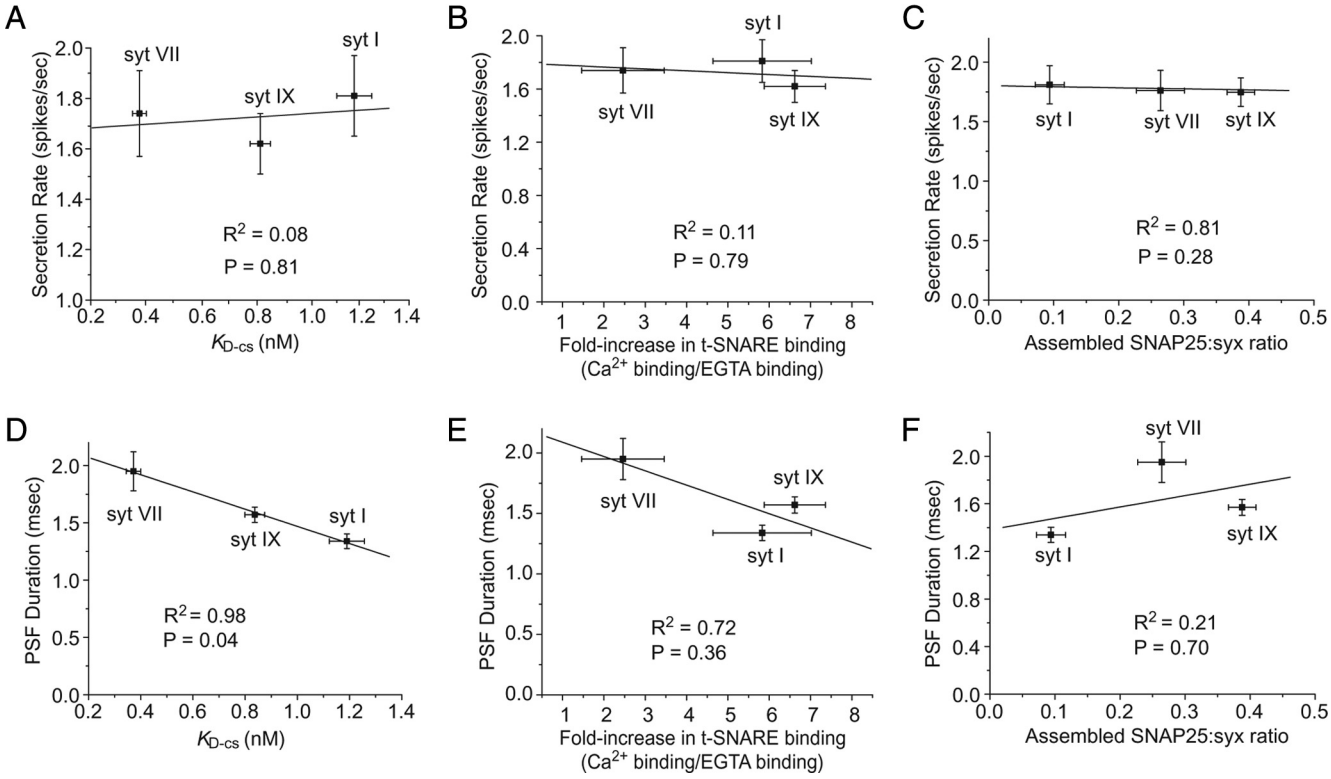

Figure 9. Test for correlation between in vitro interactions and exocytosis for syt I isoforms. As in Figure 8 secretion rate and PSF lifetime are plotted versus PS-liposome binding, t-SNARE binding, and SNARE assembly, and again as in Figure 8, a statistically significant correlation was found only for PSF duration versus K_D-cs (D).

this finding to other Ca^{2+}-sensing syt isoforms, as well as to mutants of syt I with very different in vitro interactions.

It is widely believed that both syt-PS binding and syt-SNARE binding play some role in exocytosis (Brunger, 2005; Chapman, 2008), but as indicated in the review of literature in the Introduction, the precise nature of these roles has been elusive. This laboratory had previously resolved two temporally distinct processes in exocytosis that are triggered by Ca^{2+} and speculated that syt-PS binding could drive one kinetic step and syt-SNARE binding could drive the other (Wang *et al*., 2006). A major goal of the present study was to test this hypothesis using a strategy of parallel analysis of in vitro interactions and exocytosis in PC12 cells. Because the mutants and isoforms selected here for study have very different effects on these interactions, these experiments allowed us to draw connections between exocytosis in intact cells and binding interactions in vitro. The present results do not support the hypothesis that syt-PS and syt-SNARE binding drive different steps. Instead, we found that syt-PS interactions function in both the overall rate of exocytosis and the rate of dilation of fusion pores. These experiments failed to reveal a clear role for syt interactions with t-SNAREs (Ca^{2+}-dependent or independent), either in the overall rate of exocytosis or in fusion pore transitions.

The results presented here support the idea that a Ca^{2+}-induced increase in the affinity of syt for PS accelerates a kinetic step leading to fusion pore opening. This step may well entail the induction of positive curvature in the inner bilayer leaflet (Martens *et al*., 2007; Hui *et al*., 2009; Zhang *et al*., 2009; Zhang and Jackson, 2010). This curvature could allow the membrane anchors of the t-SNAREs in the plasma membrane and v-SNAREs in the vesicle membrane to approach one another more closely and form a proteinaceous fusion pore without bringing large areas of the plasma membrane and vesicle membrane into close proximity. Energy released by Ca^{2+}-stimulated syt binding to PS could thus perform the work of opening fusion pores. Once open, syt-PS interactions will stabilize the open fusion pore by slowing its transition to a dilating state.

This view of the role for syt-PS interactions based on the manipulations of syt agrees with results obtained by manipulating PS levels (Zhang *et al*., 2009). This recent study showed that increasing PS levels by a variety of methods accelerated the overall rate of exocytosis and stabilized fusion pores by reducing k_d. In fact, changing syt-PS binding and changing PS levels both produced large significant reductions in k_d and small insignificant reductions in k_c. The fact that perturbing the syt-PS interaction using two complementary approaches altered the overall rate of fusion and the kinetics of fusion pores in a consistent manner strongly supports the hypothesis for a role in exocytosis of Ca^{2+}-dependent binding of syt to PS-containing membranes.

While our results have increased our understanding of how syt-PS interactions function in exocytosis, the role of syt-SNARE interactions remains unclear. Previous work showed that lengthening the linker between the C2A and C2B domains of syt I selectively impaired SNARE binding. The rate of linker mutant binding to PS-containing liposomes remained similar to that of wild-type syt I (Bai *et al*., 2004). However, more recent investigations of the linker mutants using protein-liposome cosedimentation indicated that lipid binding was in fact reduced (Hui and Chapman, unpublished). This discrepancy arises from the fact that equilibrium and kinetic measurements provide information about different phases of syt-PS binding (Hui *et al*., 2009). These new results indicate that it will be difficult to test the

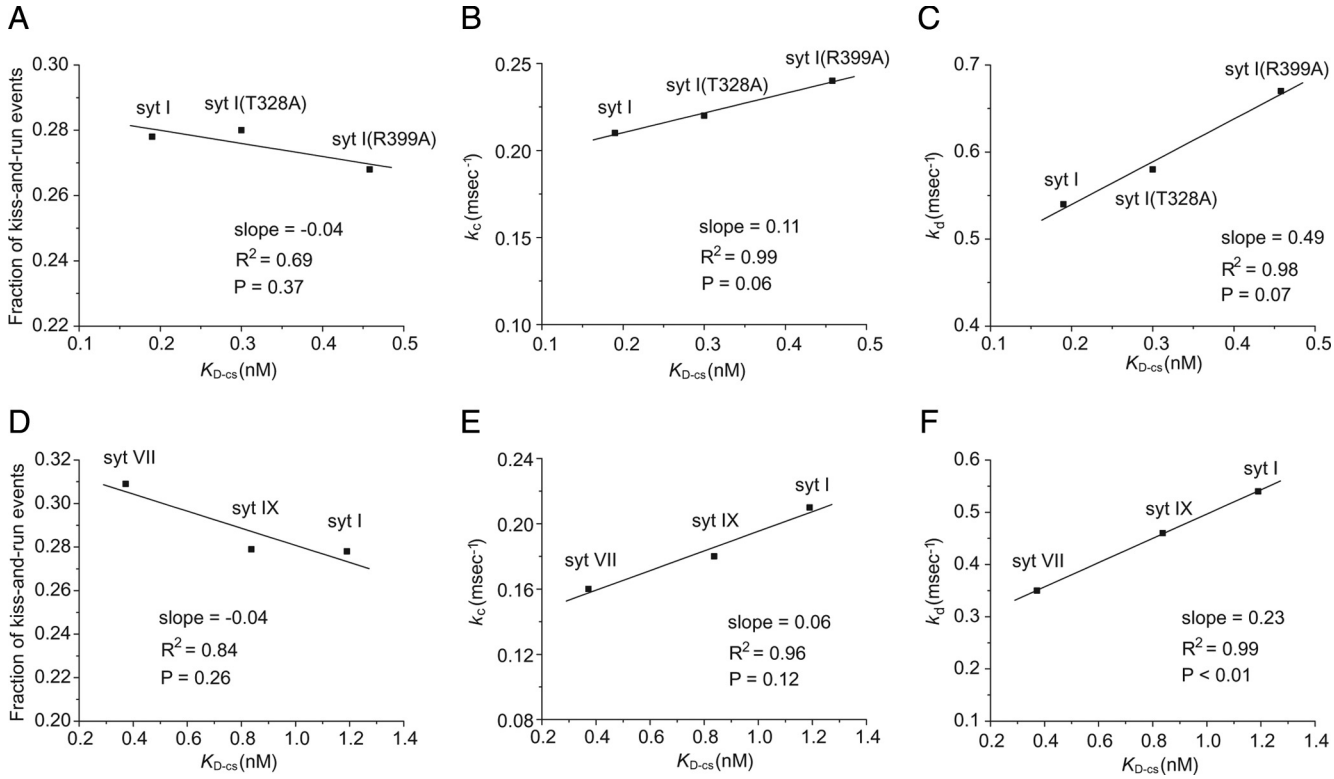

Figure 10. Plots of fusion pore kinetic parameters versus PS-liposome binding (K_D-cs) for mutations (A–C) and isoforms (D–F). The fraction of kiss-and-run event and PSF duration were used to calculate the fusion pore kinetic rate constants k_c and k_d. Only the plots of k_d versus K_D-cs yielded statistically significant correlations (F). The plots of k_d (C and F) had the steepest slopes.

role of syt-SNARE interactions. A function for syt-SNARE interactions remains a possibility, but our results suggest that if syt-PS interactions and syt-SNARE interactions are both altered, the alteration of the syt-PS interaction will dominate in the regulation of exocytosis.

A number of factors must be considered when comparing in vitro protein-protein interaction data with functional data from cells. Our lipid and SNARE binding assays must be performed with the cytoplasmic portion of syt (C2AB), and although this truncated protein functions in Ca^{2+}-triggered SNARE-mediated liposome fusion (Tucker *et al*., 2004; Bhalla *et al*., 2008), different binding properties of the truncated and full-length protein remain a possibility. Furthermore, the binding assays are equilibrium measurements and cannot detect more subtle kinetic changes in the molecular interactions. Interactions between syts and SNARE proteins other than syntaxin 1 and SNAP-25 could lead to differences between in vitro activity and function in cells. However, syt I stimulates fusion less effectively when SNAREs other than those tested here are reconstituted into liposomes (Bhalla *et al*., 2008). Nevertheless, the large number of molecules present in living cells that interact with the exocytotic apparatus provide many ways in which a protein's function in cells could diverge from its activity in vitro. Although the overexpressed proteins did not alter the expression of other major proteins involved in exocytosis (Supplemental Figure 1), the levels of some other molecules could change. Finally, one must also consider differences in the stoichiometry of the protein-protein interactions in vitro, as well as differences in local concentrations of molecules on vesicles or sequestered into the fusion machinery. These considerations together with the present results thus indicate that a role for syt-SNARE interactions in exocytosis will be difficult to demonstrate.

Overexpressing either of the two major endogenous syt isoforms of PC12 cells, syt I and syt IX (Tucker *et al*., 2003), increased the fusion pore lifetime over that of control cells (Figure 3E). Overexpressing syt VII also increased fusion pore lifetime. The only wild-type syt isoform that reduced the lifetime of a PSF was syt IV, an inhibitory isoform that does not bind Ca^{2+} (Wang *et al*., 2001). It may be that overexpressing the other isoforms overwhelms the effects of the trace levels of syt IV present in control PC12 cells (Tucker *et al*., 2003; Ahras *et al*., 2006; Zhang *et al*., 2010). Another intriguing possibility is that fusion pores are sensitive to the levels of Ca^{2+}-binding syts. Thus, the number of syt proteins that participate in unitary fusion events can increase as syt levels rise. Syt I is the most abundant syt isoform in neurons and plays a central role in rapid synchronous neurotransmitter release (Augustine, 2001; Koh and Bellen, 2003; Chapman, 2008). It is thus significant that among the syt isoforms, syt I overexpression produced the fastest rate of fusion pore dilation (Figure 10F). This will allow fusion pores to advance more rapidly to a dilating state compared with syt VII or syt IX. This property thus makes syt I well adapted for rapid release.

ACKNOWLEDGMENTS

This work was funded by National Institutes of Health grants NS44057 (to M.B.J.) and MH61876 (to E.R.C.). E.R.C. is an investigator of the Howard Hughes Medical Institute.

REFERENCES

Ahras, M., Otto, G. P., and Tooze, S. A. (2006). Synaptotagmin IV is necessary for the maturation of secretory granules in PC12 cells. J. Cell Biol. *173*, 242–251.

Augustine, G. J. (2001). How does calcium trigger neurotransmitter release? Curr. Opin. Neurobiol. *11*, 320–326.

Bai, J., Wang, C. T., Richards, D. A., Jackson, M. B., and Chapman, E. R. (2004). Fusion pore dynamics are regulated by synaptotagmin*t-SNARE interactions. Neuron *41*, 929–942.

Bennett, M. K., Calakos, N., and Scheller, R. H. (1992). Syntaxin: a synaptic protein implicated in docking of synaptic vesicles at presynaptic active zones. Science *257*, 255–259.

Bhalla, A., Chicka, M. C., and Chapman, E. R. (2008). Analysis of the synaptotagmin family during reconstituted membrane fusion. Uncovering a class of inhibitory isoforms. J. Biol. Chem. *283*, 21799–21807.

Bhalla, A., Chicka, M. C., Tucker, W. C., and Chapman, E. R. (2006). Ca(2+)-synaptotagmin directly regulates t-SNARE function during reconstituted membrane fusion. Nat. Struct. Mol. Biol. *13*, 323–330.

Bhalla, A., Tucker, W. C., and Chapman, E. R. (2005). Synaptotagmin isoforms couple distinct ranges of Ca2+, Ba2+, and Sr2+ concentration to SNARE-mediated membrane fusion. Mol. Biol. Cell *16*, 4755–4764.

Brose, N., Petrenko, A. G., Sudhof, T. C., and Jahn, R. (1992). Synaptotagmin: a calcium sensor on the synaptic vesicle surface. Science *256*, 1021–1025.

Brunger, A. T. (2005). Structure and function of SNARE and SNARE-interacting proteins. Q. Rev. Biophys. *38*, 1–47.

Chapman, E. R. (2008). How does synaptotagmin trigger neurotransmitter release? Annu. Rev. Biochem. *77*, 615–641.

Chapman, E. R., and Jahn, R. (1994). Calcium-dependent interaction of the cytoplasmic region of synaptotagmin with membranes. Autonomous function of a single C2-homologous domain. J. Biol. Chem. *269*, 5735–5741.

Chow, R. H., and von Rüden, L. (1995). Electrochemical detection of secretion from single cells. In: Single-Channel Recording, eds. B. Sakmann, Neher, E., New York: Plenum Press, 245–275.

Craxton, M. (2007). Evolutionary genomics of plant genes encoding N-terminal-TM-C2 domain proteins and the similar FAM62 genes and synaptotagmin genes of metazoans. BMC Genomics *8*, 259.

Davletov, B. A., and Sudhof, T. C. (1993). A single C2 domain from synaptotagmin I is sufficient for high affinity Ca2+/phospholipid binding. J. Biol. Chem. *268*, 26386–26390.

Fernandez-Chacon, R., Konigstorfer, A., Gerber, S. H., Garcia, J., Matos, M. F., Stevens, C. F., Brose, N., Rizo, J., Rosenmund, C., and Sudhof, T. C. (2001). Synaptotagmin I functions as a calcium regulator of release probability. Nature *410*, 41–49.

Fernandez-Chacon, R., Shin, O. H., Konigstorfer, A., Matos, M. F., Meyer, A. C., Garcia, J., Gerber, S. H., Rizo, J., Sudhof, T. C., and Rosenmund, C. (2002). Structure/function analysis of Ca2+ binding to the C2A domain of synaptotagmin 1. J. Neurosci. *22*, 8438–8446.

Fernandez, I., Arac, D., Ubach, J., Gerber, S. H., Shin, O., Gao, Y., Anderson, R. G., Sudhof, T. C., and Rizo, J. (2001). Three-dimensional structure of the synaptotagmin 1 C2B-domain: synaptotagmin 1 as a phospholipid binding machine. Neuron *32*, 1057–1069.

Fukuda, M., Kanno, E., Satoh, M., Saegusa, C., and Yamamoto, A. (2004). Synaptotagmin VII is targeted to dense-core vesicles and regulates their Ca2+-dependent exocytosis in PC12 cells. J. Biol. Chem. *279*, 52677–52684.

Gaffaney, J. D., Dunning, F. M., Wang, Z., Hui, E., and Chapman, E. R. (2008). Synaptotagmin C2B domain regulates Ca2+-triggered fusion in vitro: critical residues revealed by scanning alanine mutagenesis. J. Biol. Chem. *283*, 31763–31775.

Hui, E., Bai, J., Wang, P., Sugimori, M., Llinas, R. R., and Chapman, E. R. (2005). Three distinct kinetic groupings of the synaptotagmin family: candidate sensors for rapid and delayed exocytosis. Proc. Natl. Acad. Sci. USA. *102*, 5210–5214.

Hui, E., Johnson, C. P., Yao, J., Dunning, F. M., and Chapman, E. R. (2009). Synaptotagmin-mediated bending of the target membrane is a critical step in Ca(2+)-regulated fusion. Cell *138*, 709–721.

Koh, T. W., and Bellen, H. J. (2003). Synaptotagmin I, a Ca2+ sensor for neurotransmitter release. Trends Neurosci. *26*, 413–422.

Lynch, K. L., Gerona, R. R., Kielar, D. M., Martens, S., McMahon, H. T., and Martin, T. F. (2008). Synaptotagmin-1 utilizes membrane bending and SNARE binding to drive fusion pore expansion. Mol. Biol. Cell *19*, 5093–5103.

Mackler, J. M., Drummond, J. A., Loewen, C. A., Robinson, I. M., and Reist, N. E. (2002). The C(2)B Ca(2+)-binding motif of synaptotagmin is required for synaptic transmission in vivo. Nature *418*, 340–344.

Martens, S., Kozlov, M. M., and McMahon, H. T. (2007). How synaptotagmin promotes membrane fusion. Science *316*, 1205–1208.

Nagy, G., Kim, J. H., Pang, Z. P., Matti, U., Rettig, J., Sudhof, T. C., and Sorensen, J. B. (2006). Different effects on fast exocytosis induced by synaptotagmin 1 and 2 isoforms and abundance but not by phosphorylation. J. Neurosci. *26*, 632–643.

Nishiki, T., and Augustine, G. J. (2004). Dual roles of the C2B domain of synaptotagmin I in synchronizing Ca2+-dependent neurotransmitter release. J. Neurosci. *24*, 8542–8550.

Pang, Z. P., Shin, O. H., Meyer, A. C., Rosenmund, C., and Sudhof, T. C. (2006). A gain-of-function mutation in synaptotagmin-1 reveals a critical role of Ca2+-dependent soluble N-ethylmaleimide-sensitive factor attachment protein receptor complex binding in synaptic exocytosis. J. Neurosci. *26*, 12556–12565.

Rhee, J. S., Li, L. Y., Shin, O. H., Rah, J. C., Rizo, J., Sudhof, T. C., and Rosenmund, C. (2005). Augmenting neurotransmitter release by enhancing the apparent Ca2+ affinity of synaptotagmin 1. Proc. Natl. Acad. Sci. USA. *102*, 18664–18669.

Shao, X., Davletov, B. A., Sutton, R. B., Sudhof, T. C., and Rizo, J. (1996). Bipartite Ca2+-binding motif in C2 domains of synaptotagmin and protein kinase C. Science *273*, 248–251.

Shao, X., Fernandez, I., Sudhof, T. C., and Rizo, J. (1998). Solution structures of the Ca2+-free and Ca2+-bound C2A domain of synaptotagmin I: does Ca2+ induce a conformational change? Biochemistry *37*, 16106–16115.

Stevens, C. F., and Sullivan, J. M. (2003). The synaptotagmin C2A domain is part of the calcium sensor controlling fast synaptic transmission. Neuron *39*, 299–308.

Travis, E. R., and Wightman, R. M. (1998). Spatio-temporal resolution of exocytosis from individual cells. Annu. Rev. Biophys. Biomol. Struct. *27*, 77–103.

Tucker, W. C., Edwardson, J. M., Bai, J., Kim, H. J., Martin, T. F., and Chapman, E. R. (2003). Identification of synaptotagmin effectors via acute inhibition of secretion from cracked PC12 cells. J. Cell Biol. *162*, 199–209.

Tucker, W. C., Weber, T., and Chapman, E. R. (2004). Reconstitution of Ca^{2+}-regulated membrane fusion by synaptotagmin and SNAREs. Science *304*, 435–438.

Wang, C. T., Bai, J., Chang, P. Y., Chapman, E. R., and Jackson, M. B. (2006). Synaptotagmin-Ca^{2+} triggers two sequential steps in regulated exocytosis in rat PC12 cells: fusion pore opening and fusion pore dilation. J. Physiol. *570*, 295–307.

Wang, C. T., Grishanin, R., Earles, C. A., Chang, P. Y., Martin, T. F., Chapman, E. R., and Jackson, M. B. (2001). Synaptotagmin modulation of fusion pore kinetics in regulated exocytosis of dense-core vesicles. Science *294*, 1111–1115.

Wang, P., Wang, C. T., Bai, J., Jackson, M. B., and Chapman, E. R. (2003). Mutations in the effector binding loops in the C2A and C2B domains of synaptotagmin I disrupt exocytosis in a nonadditive manner. J. Biol. Chem. *278*, 47030–47037.

Zhang, Z., Hui, E., Chapman, E. R., and Jackson, M. B. (2009). Phosphatidylserine regulation of Ca^{2+}-triggered exocytosis and fusion pores in PC12 cells. Mol. Biol. Cell *20*, 5086–5095.

Zhang, Z., and Jackson, M. B. (2008). Temperature dependence of fusion kinetics and fusion pores in Ca2+-triggered exocytosis from PC12 cells. J. Gen. Physiol. *131*, 117–124.

Zhang, Z., and Jackson, M. B. (2010). Membrane bending energy and fusion pore kinetics in Ca2+-triggered exocytosis. Biophys. J. *98*, 2524–2534.

Zhang, Z., Zhang, Z., and Jackson, M. B. (2010). Synaptotagmin IV modulation of vesicle size and fusion pores in PC12. Biophys. J. *98*, 968–978.